An adjustable linear Halbach array

J.E. Hilton, S.M. McMurry

PII: S0304-8853(12)00100-X
DOI: doi:10.1016/j.jmmm.2012.02.014
Reference: MAGMA57359

To appear in: *Journal of Magnetism and Magnetic Materials* www.elsevier.com/locate/jmmm

Received date: 16 November 2011
Revised date: 25 January 2012

Cite this article as: J.E. Hilton and S.M. McMurry, An adjustable linear Halbach array, *Journal of Magnetism and Magnetic Materials,* doi:10.1016/j.jmmm.2012.02.014

An adjustable linear Halbach array

J. E. Hilton[a,*], S. M. McMurry[b]

[a] *CSIRO Mathematics, Informatics and Statistics, Clayton South, VIC 3169, Australia*
[b] *School of Physics, Trinity College Dublin, Ireland*

Abstract

The linear Halbach array is a well known planar magnetic structure capable, in the idealized case, of generating a one-sided magnetic field. We show that such a field can be created from an array of uniformly magnetized rods, and rotating these rods in an alternating fashion can smoothly transfer the resultant magnetic field through the plane of the device. We examine an idealized model composed of infinite line dipoles and carry out computational simulations on a realizable device using a magnetic boundary element method. Such an arrangement can be used for an efficient latching device, or to produce a highly tunable field in the space above the device.

Keywords:
Magnetic field, Permanent magnet flux source, Halbach array, Simulation

1. Introduction

Applications requiring specifically tailored magnetic fields are widespread in industry and research. The field sources for such applications come in a diverse variety of shape and form, but can be approximately divided into pow-

*Corresponding author
Email address: James.Hilton@csiro.au (J. E. Hilton)

ered and static categories. Powered sources use electromagnets, which require an electric current to create the field. Static sources consist of arrangements of permanently magnetized hard magnetic material, possibly augmented with softer magnetic materials (Coey, 2002). Although far higher field strengths can be reached with electromagnetic sources, static sources have the natural advantage that they require no continuous input of energy.

The discovery in the 1970's of magnetic materials with both high coercivity and remanence, such as SmCo and NdFeB compounds, spurred development of static field sources as a viable alternative to powered field sources. Of these an important subset are designs based on particular arrangement of permanent magnetic sources known as a 'Halbach array', or a 'flux sheet'. The first such design was described by Mallinson (Mallinson, 1973) as a sheet of magnetic material with an alternating magnetization pattern. This particular magnetization pattern gave the design the unique, and counter-intuitive, ability to confine the magnetic field to only one side of the sheet. Continuous distributions of this pattern are shown in Figs. 1a and 1b, along with a schematic representation of the resulting field. As the field is augmented on one side and canceled on the other, the resultant field is effectively doubled on the augmented side. Mallinson showed the field would be confined in this manner if the components of magnetization were any Hilbert transform pair, the simplest of which is $\mathbf{m} = \sin(x)\hat{\mathbf{i}} + \cos(x)\hat{\mathbf{j}}$, where $\mathbf{m}$ is the magnetization vector and x the position along the sheet. A familiar example of such a magnetization pattern is found in the polymer loaded ferrite material on the back of fridge magnets. Such magnetic devices are now also widely used in 'wiggler' magnets in free electron lasers and synchrotrons (Juanhuix and

Traveria, 1998), far from the 'magnetic curiosity' Mallinson described in his original paper.

Rolling up such a flux sheet into a cylinder gives a field source known as a 'Halbach cylinder', which was discovered independently by Klaus Halbach during investigations into magnetic systems for particle accelerators (Halbach, 1980). These remarkable designs can give a uniform, or multi-polar field, confined entirely within the cylindrical bore of the design. Many configurations and permutations of such cylinder designs are possible. Nesting two Halbach cylinders allows a variable field within the bore of the device, which can be precisely controlled by the relative angle between the two cylinders (Ni Mhiochain, 1999). The magnetization distribution required for a Halbach array can, remarkably, even be created by induced magnetization in a highly permeable soft magnetic material (Peng, 2003). An idealized infinite length Halbach cylinder produces an entirely uniform homogeneous field within the bore of the cylinder. However, realizable designs suffer from 'end effects' due to finite length, which reduces the field homogeneity within the bore. Methods such as shimming and shaping the geometry (Hilton, 2007) can correct this, significantly improving the uniformity of the field within such finite length cylindrical designs.

Replacing the individual magnetic segments of a Halbach cylinder with transversely magnetized rods allows the field within the bore of the design to be controlled by the relative rotation of each rod. This design, called a 'magnetic mangle' was first suggested and investigated by Cugat (Cugat et al., 1994). In this study we investigate a variation of this design in which an array of permanent magnetic rods, transversely magnetized perpendicular to

the cylindrical axes, are arranged into a linear Halbach array. Rotating each element of the array in the opposite direction to the neighboring elements is shown to smoothly transfer the magnetic field from one side of the array to the other. In a similar manner to how a linear Halbach array can be considered an 'opened' Halbach cylinder, the structure investigated here can be understood as an 'opened' magnetic mangle design. Although a wide range of tunable field sources exist (Coey, 2002; Bjørk et al., 2010), including designs based on movable Halbach arrays, this design appears to have been overlooked. Arrangements of this design producing fields above and below the plane of the rods are shown schematically in Figs. 1c and 1d, respectively.

In the following sections, we first investigate an idealized model of the device using an array of infinite line dipoles. The resultant torques and energy of each dipole are evaluated in order to asses the practicalities of any such device. Then a finite size, realizable device is computationally modeled using a magnetic boundary element method. We show that such a device produces a strong, switchable magnetic field in the space above the device and is not subject to excessive torques. Finally, we suggest a practical design for such a device based on a simple gearing arrangement.

2. Modelling of the design

2.1. An array of magnetic line dipoles

The arrangement shown in Fig. 1c and 1d can be modeled, to a first approximation, as a sequence of line dipoles. This basic model allows the investigation of field and torque behavior on the dipoles as they are rotated relative to each other. We use the magnetic scalar potential, $H(\mathbf{r}) = -\nabla\psi(\mathbf{r})$

for a magnetic point dipole in Cartesian space, with unit vectors $\hat{\mathbf{i}}$, $\hat{\mathbf{j}}$, and $\hat{\mathbf{k}}$ in the x, y and z directions, respectively. This is given by:

$$\psi(\mathbf{r}) = \frac{\mathbf{m} \cdot \mathbf{r}}{4\pi|\mathbf{r}|^3} \tag{1}$$

where $\mathbf{m}$ is the point dipole moment. For a line dipole, confined to the $x-y$ plane and extending to $\pm\infty$ in the z direction, this becomes:

$$\int_{-\infty}^{\infty} \frac{\mathbf{m} \cdot \mathbf{r}}{4\pi|\mathbf{r}|^3} dz = \frac{\boldsymbol{\lambda} \cdot \mathbf{r}}{4\pi|\mathbf{r}|^2} \tag{2}$$

where $\boldsymbol{\lambda}$ is the line dipole moment. The magnetic field of a line dipole is significantly different to that of a point dipole. In polar co-ordinates the field magnitude of a line dipole is independent of the polar angle to the dipole, unlike a point dipole (Cugat et al., 1994). This effect is exploited in arrangements such as this to provide the augmentation and cancellation of the field on opposite sides of the plane of the dipoles. The scalar potential from a collection of N such dipoles is given by:

$$\psi(\mathbf{r}) = \frac{1}{4\pi} \sum_{a=1}^{N} \frac{\boldsymbol{\lambda}_a \cdot (\mathbf{r} - \mathbf{r}_a)}{|(\mathbf{r} - \mathbf{r}_a)|^2} \tag{3}$$

where $\mathbf{r}_a$ is the position of dipole a and the line dipole moment, in this case, is given by:

$$\boldsymbol{\lambda}_a(\phi) = \lambda \left(\sin[(-1)^a \phi - \frac{a\pi}{2}] \hat{\mathbf{i}} + \cos[(-1)^a \phi - \frac{a\pi}{2}] \hat{\mathbf{j}} \right) \tag{4}$$

where ϕ is an overall rotation of the dipoles in the structure. It should be noted that the rotational dependency on ϕ for each dipole is opposite to that of the neighboring dipoles due to the factor $(-1)^a$ in Eq. (4). We consider an

arrangement where the dipoles are evenly spaced along the x axis, separated by a distance l. This gives a final expression for the magnetic scalar potential as:

$$\psi(\mathbf{r},\phi) = \frac{1}{4\pi}\sum_{a=1}^{N}\frac{\boldsymbol{\lambda}_a\cdot(\mathbf{r}-al\hat{\mathbf{i}})}{|(\mathbf{r}-al\hat{\mathbf{i}})|^2} \tag{5}$$

The torque on each dipole at rotation angle ϕ is an important measure of the practicality of any device based on this design. The torque on dipole b, τ_b, from the dipole array can be evaluated from Eq. (5) as:

$$\tau_b(\phi) = -\frac{1}{4\pi}\boldsymbol{\lambda}_b\times\nabla\sum_{a=1,a\neq b}^{N}\frac{\boldsymbol{\lambda}_a\cdot(\mathbf{r}-al\hat{\mathbf{i}})}{|(\mathbf{r}-al\hat{\mathbf{i}})|^2} \tag{6}$$

where the torque vector is aligned with the z axis. The energy of each dipole allows the stability of the dipole at a particular rotation angle to be investigated. The energy of a dipole in a field is given by $U=-\boldsymbol{\lambda}\cdot\mathbf{H}/\mu_0$, so the energy of a dipole b in the array is:

$$U_b(\phi) = -\frac{1}{4\pi\mu_0}\boldsymbol{\lambda}_b\cdot\nabla\sum_{a=1,a\neq b}^{N}\frac{\boldsymbol{\lambda}_a\cdot(\mathbf{r}-al\hat{\mathbf{i}})}{|(\mathbf{r}-al\hat{\mathbf{i}})|^2} \tag{7}$$

2.2. Magnetized finite length segments

In order to investigate the practicalities of an actual magnetic device, the arrangement was computationally modeled as a sequence of rods of hard magnetic material, uniformly magnetized perpendicular to the cylindrical axis. The fields from these arrangements were calculated using a magnetic boundary element method based on the magnetic charge model (Hilton, 2007). The surface of each rod was decomposed into triangular sheets of magnetic charge, for which an analytical solution exists. The field at any point was calculated

as the summation of the fields from each of these sheets. The method has been applied to a wide range of similar magnetic structures, and has been carefully validated against existing analytical field solutions, as well as experimental measurements of new magnetic designs (Hilton, 2007). The torque on each magnet in the design can likewise be calculated from the torque on each triangular charge sheet about the center of mass of each magnet. The torque calculations have been verified by comparison to experimentally measured torques (Ni Mhiochain, 1999) on complex magnetic structures.

3. Results

3.1. Field and torque of the dipole array

The expression for the array of infinite line dipoles was solved using the computational package Mathematica. For convenience, the constant $\lambda/4\pi$ and the dipole spacing, l, were both set to unity. The resulting scalar potential for a array of 65 line dipoles is shown in Fig. 2 at three rotation angles. The field clearly reverses from above to below the plane of the line dipoles as the dipoles are rotated alternately clockwise and anticlockwise as ϕ is changed from 0 through to $\pi/2$ radians. The asymmetry in the scalar potential is caused by end effects due to the finite number of dipoles in the array. The scalar potential is symmetrical at $\phi = \pi/4$ as the dipoles are arranged in pairs orientated at $\pm\pi/4$ radians to the vertical.

The field magnitude, $|\mathbf{H}|$, along a line parallel to the x-axis at a position $y = 2$ is shown in Fig. 3 for a range of ϕ. It should be noted that the low values for $|\mathbf{H}|$, in comparison to real-world magnetic structures, are due to the choices of $\lambda = 4\pi$ and $l = 1$. This has no bearing on the following

discussion of the results, as we are concerned with only the form of the field within this section. Oscillatory effects from the finite number of dipoles are apparent at the start and end of the array, but the field magnitude over the mid part is approximately uniform. Rotation of the array, surprisingly, does not appear to affect the uniformity of the field magnitude, which smoothly reduces to zero as each dipole in the array is alternately rotated through $\phi = 0 \rightarrow \pi/2$ radians. At $\phi = \pi/2$ radians the field magnitude at $y = 2$ is reduced to zero.

The H_y field component at the mid point of the array, $x = 32$, at a position $y = 2$ is shown in Fig. 4 for $\phi = 0 \rightarrow \pi$. The x-component of the field, $H_x \sim 0$ at this point for the entire range of ϕ. The y-component smoothly varies as the cosine of the rotation angle, ϕ. The field is zero at $\phi = \pi/2$, as shown in Fig. 3, but reverses in the range $\pi/2 \rightarrow \pi$

Torques on each dipole in the array were calculated from Eq. (6) and are plotted against dipole position in Fig. 5. The effect of the finite number of dipoles is again apparent at the start and end of the array. However, the torque rapidly reaches a fixed value for dipoles only several steps from the ends of the array. The torque on each dipole varies as the sine of the rotation angle, reaching a maximum value at $\phi = \pi/4$, and is approximately zero over the bulk of the array at $\phi = 0, \pi/2$.

The energy of each dipole in the array was calculated from Eq. (7) and is plotted against dipole position in Fig. 6 for $\phi = 0, \pi/2$. At $\phi = \pi/4$, all dipoles have approximately zero energy. The energy minimum of a dipole at $\phi = 0$ or $\phi = \pi/2$ was found to occur at the energy maxima of its neighboring dipoles. The torques on each dipole in the array at $\phi = 0, \pi/2$ are zero,

showing that the dipoles are alternately at stable and unstable mechanical equilibria at these orientations.

A series of line dipoles therefore shows the desired behavior, producing a field which varies as $H_y \sim \cos(\phi)$. The largest torques are experienced by the dipoles within the stray field regions at the ends of the array. The torques within the bulk of the array are approximately zero for $\phi = 0$ and $\phi = \pi/2$. However, each dipole at these orientations is either at an energy minimum or maximum with respect to its neighboring dipoles, showing that mechanical stabilization of the array is necessary for a practical device.

3.2. Field and torque of a magnetic rod arrangement

In the simple dipole model, end effects caused by the finite number of dipoles were observed at the start and ends of the array. Practical magnetic designs also suffer from additional effects caused by the finite length of the magnetic components in the design (Ni Mhiochain, 1999; Bjørk , 2011). These can decrease both the effective magnetic field and the homogeneity of the field over the working area of the device. To investigate these effects in a realizable device, a practical sized magnetic design was modeled. Sixteen transversely magnetized rods were used in the device, $N = 16$, with a remnant magnetization of $B_r = 1.2T$, typical of a standard grade of the hard magnetic material NdFeB. The rods were chosen to be 10 cm long, with diameter 1 cm, separated by an air gap of 2.5 mm between each rod. The circular cross-section of each rod was discretized into a 20 sided regular polygon, and the magnetic charge on each element was calculated from the dot product of the element and the magnetization distribution within the rod, given by Eq. (4).

The magnetic flux density, $|\mathbf{B}|$, from the arrangement is shown in Fig. 7, where only half the design is shown as the field is symmetrical about the y axis. As expected, the field reverses as each rod is rotated alternately through $\phi = 0 \rightarrow \pi/2$. The magnitude of the field at $\phi = 0, \pi/2$ is reasonably uniform and homogeneous within central part of the design, even for such an arrangement consisting of only 16 rods.

The flux density, $|\mathbf{B}|$, along a line parallel to the x-axis at $y = 2\ cm$ is shown in Fig. 8 for $\phi = 0, \pi/4, \pi/3, \pi/2$. The end of the array is at approximately $x = 10\ cm$. The field profile at $\phi = 0$ is similar to the array of line dipoles, consisting of a constant field over the central part of the array with an oscillatory stray field at the ends of the device. The field at $y = 2\ cm$ shows almost an ideal reduction from 75 mT to zero as the magnetic segments are rotated.

The torque on four rods in the design is shown in Fig. 9, where the torque is evaluated about the center of mass of the rod. The four rods are labeled in Fig. 7a as $n = 1, 2, 3, 4$. The torque on each rod varies sinusoidally with rotation angle ϕ, as found in the simplified line dipole model. Similarly, the rods experiencing the maximum torques are located at the ends of the array.

The magnetic rod model therefore qualitatively agrees with the basic line dipole model, showing the same field and torque variations with rotation angle, ϕ.

3.3. Variation of the geometry for the magnetic rod arrangement

The design can be readily optimized, as the field shows a non-linear dependency on rod separation. The flux density, $|\mathbf{B}|$, from the arrangement with rod separations of a) 50 mm and b) 75 mm are shown in Fig. 10, for

$\phi = 0$. Increasing the rod separation does not affect the field homogeneity in the central region above the plane of the rods, and appears to slightly increase the maximum magnetic field strength away from the plane of the rods. A plot of the flux density against separation is shown in Fig. 11 at $x = 0$ for several values of y. At large rod separations, $|\mathbf{B}| \to 0$. The vertical dashed line shows the 25 mm separation used in the preceding section. It can be seen that the optimal spacing, giving the maximum field strength, at any chosen vertical position above the rods varies with the vertical position.

4. Discussion

The magnetic field strength in the plane above a flux sheet is given, in the idealized case, by $|B|^2 = Ke^{-ky}$ (Mallinson, 1973). As the field varies with the cosine of the rotation angle, the field in an arrangement of magnetized rods can therefore be approximated by $|B|^2 = K'e^{-k'y}\cos^2(\phi)$, where K', k' are constants depending on the magnetic remanence, rod separation and other geometric factors. For the design discussed in the previous section, with $N = 16$ and a rod separation of 25 mm, these constants were found from data fitting to be $K' = 0.923, k' = 256$ for $y > 1$ cm. The field was very close to the expected exponential form, with the natural logarithm of the exponential fit having $R^2 = 0.9998$. For designs with N rods, the field was found to be relatively invariant for $N > 16$, with $< 1\%$ difference in the measured field at $y = 2$ cm compared between designs with $N = 16$ and $N = 64$. The field at $y = 2$ cm and the percentage difference in the field in comparison to a design with $N = 16$ is given in Table 1 for a selection of N, along with the associated fitting parameters K' and k'.

N	$\lvert\mathbf{B}\rvert_{y=2\ cm}$	$\Delta\lvert\mathbf{B}\rvert\%$	K'	k'
16	5.635	0	0.923	256.0
24	5.668	0.582	0.866	252.1
32	5.674	0.691	0.855	251.3
64	5.677	0.741	0.850	250.9

Table 1: Flux density $|\mathbf{B}|$ at $y = 2\ cm, \phi = 0$ for various N, % difference in $|\mathbf{B}|$ from a design with $N = 16$ and fitting parameters K', k'.

Simulations show that such a design is easily realizable and will not be subject to excessive torques during rotation on each of the rods. Mechanical stabilization is required, however, as no global energy minima exist for the system. Rods at energy minima, and stable mechanical equilibrium, have neighbors at energy maxima at unstable equilibria. A very straightforward solution exists, however, giving both mechanical stabilization as well as allowing the ability to rotate rods alternately. This is simply to use an equal gearing of each rod to the neighboring rod, as shown in Fig. 12. It can be noted that a flux sheet can be discretized into more sections to give a magnetization pattern which varies more smoothly (Bjørk et al., 2010), but this would require a far more complex gearing mechanism.

Such a design can be used for a range of practical applications. For example, the latching strength of such a device varies with the cosine squared of the rotation angle ϕ. This can be shown by evaluating the Maxwell stress tensor in the idealized case of a highly permeable soft magnetic material parallel to the plane of the rods. The latching strength for each pole in the device is then given by $F_{latch} = NB_y^2 A/4\mu_0$ (Furlani, 2001), where N is the number of rods and A is the total area of the design. As $B_y \sim \cos(\phi)$ for this

device, this gives $F_{latch} \sim N\cos^2(\phi)A/4\mu_0$. For the design in the preceding section with a rod separation of 25 mm, this gives a maximum latch strength on a soft magnetic plate at $y = 2\ cm$ of $F_{latch} \sim 180N$, which smoothly varies to zero as the rods are rotated.

5. Conclusion

A series of magnetized rods, arranged in the form of Mallinson's flux sheet, produces a field confined to one side of the plane of the rods. The field can be transferred through the plane by alternating rotation of each rod. Such an arrangement can be fabricated into a practical device by a simple gearing arrangement, as shown schematically in Fig. 12. Such a device would have a range of applications, such as a mechanical magnetic latching or a variable field source. Two such parallel arrangements might be used as a variable wiggler magnet for free electron laser and synchrotron devices. It is our hope that this simple design, which appears to have been previously overlooked, will be a useful addition to the family of tunable field source devices.

J. M. D. Coey, Permanent magnet applications, Journal of Magnetism and Magnetic Materials 248 (2002), 441-456.

J. C. Mallinson, One-Sided Fluxes A Magnetic Curiosity? IEEE Transactions on Magnetics, 9 (1973), 678-682.

J. Juanhuix, M. Traveria, Magnetic design and light characteristics of a Wiggler for the LLS, 6th European Particle Accelerator Conference, Stockholm, Sweden, Jun 1998, 2228.

K. Halbach, Design of permanent multipole magnets with oriented rare earth cobalt material, Nuclear Instruments and Methods 169(1) (1980), 110.

T. R. Ni Mhiochain, D. Weaire, S. M. McMurry, J. M. D. Coey, Analysis of torque in nested magnetic cylinders, Journal of Applied Physics, 86 (1999), 64126424

J. E. Hilton, S. M. McMurry, Halbach cylinders with improved field homogeneity and tailored gradient fields, IEEE Transactions on Magnetics 43(5) (2007), 1898-1902.

Q. Peng, S. M. McMurry, J. M. D. Coey, Cylindrical permanent-magnet structures using images in an iron shield, IEEE Transactions on Magnetics 39(4) (2003), 19831989.

O. Cugat, P. Hansson, J. D. M. Coey, Permanent Magnet Variable Flux Sources, IEEE Transactions on Magnetics 30(6) (1994) 4602-4604.

R. Bjørk, C. R. H. Bahl, A. Smith, N. Pryds, Comparison of adjustable permanent magnetic field sources, Journal of Magnetism and Magnetic Materials 322 (2010) 36643671.

R. Bjørk, The ideal dimensions of a Halbach cylinder of finite length, Journal of Applied Physics 109 (2011), 013915

E. P. Furlani, Permanent magnet and electromechanical devices: materials, analysis, and applications, Academic Press, 2001.

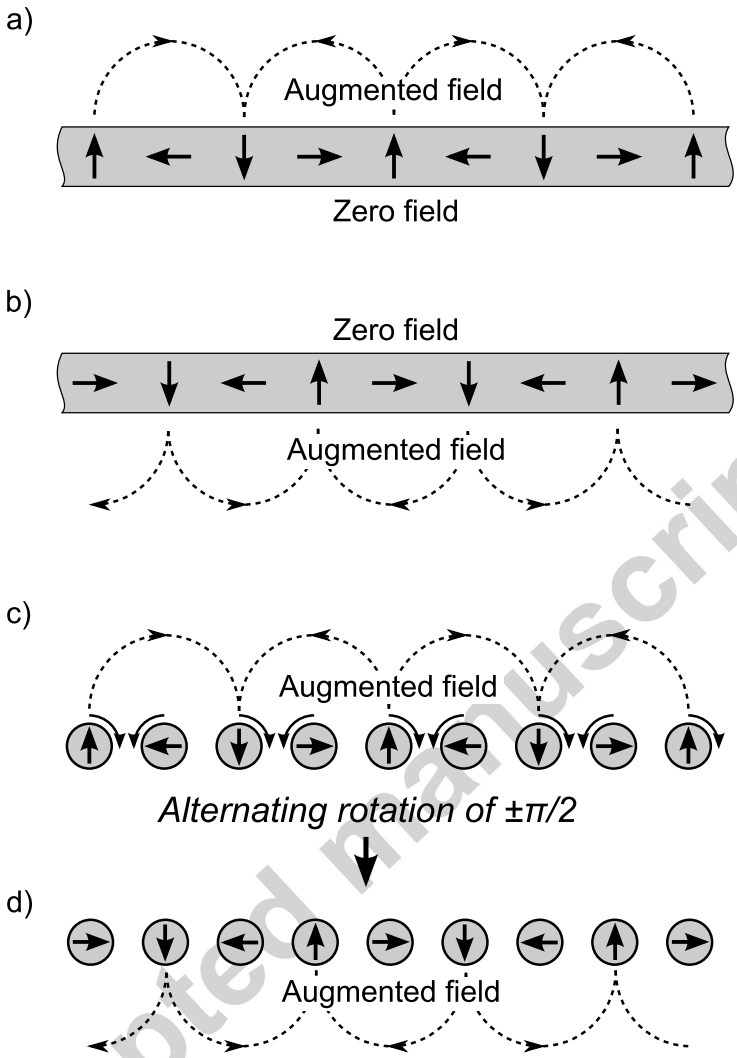

Figure 1: a) Continuous magnetization pattern generating a one-sided field above the plane of the magnet. b) Continuous magnetization pattern generating a one-sided field below the plane of the magnet. c) Discretization of the continuous distribution generating a field above the plane of the magnet. d) Discretization of the continuous distribution generating a field below the plane of the magnet. Alternating clockwise and anti-clockwise rotation of each rod reverses the one-sided field from above to below the plane.

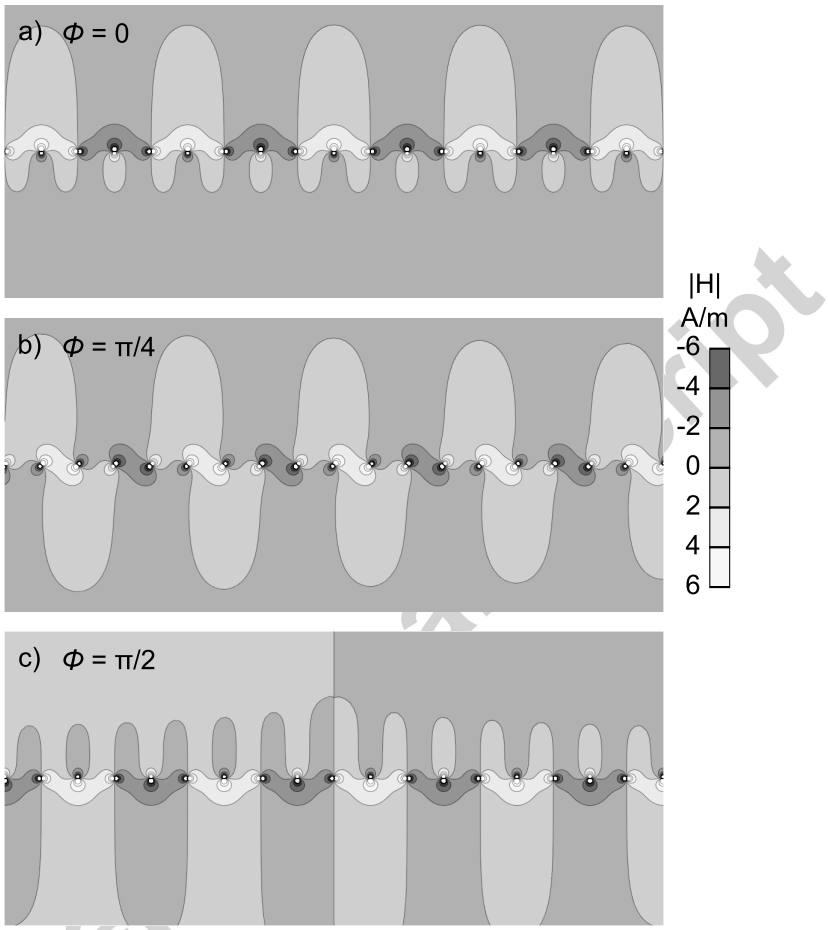

Figure 2: Contours of magnetic scalar potential for a element array of line dipoles, with rotations a) $\phi = 0$, b) $\phi = \pi/4$ and c) $\phi = \pi/2$ radians.

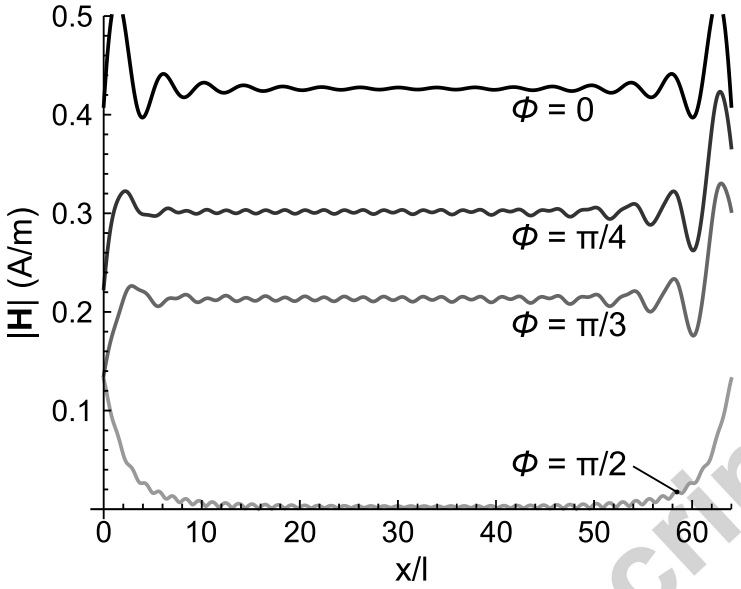

Figure 3: Field magnitude $|\mathbf{H}|$ against x along a line at $y = 2$, parallel to the x-axis, at rotation angles $\phi = 0, \pi/4, \pi/3, \pi/2$ radians.

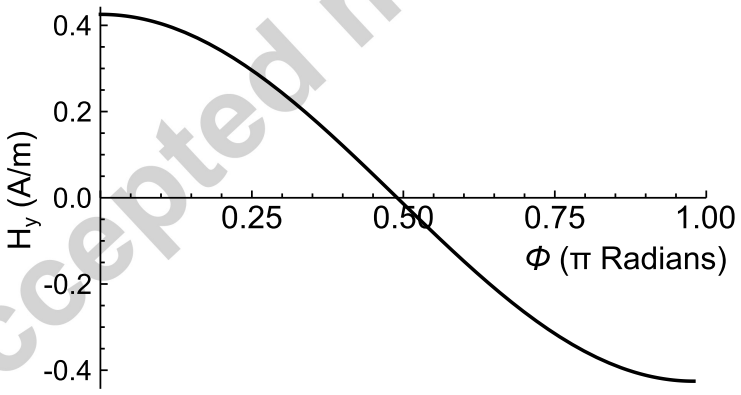

Figure 4: Field component H_y at $y = 2$ in center of array as a function of rotation angle ϕ.

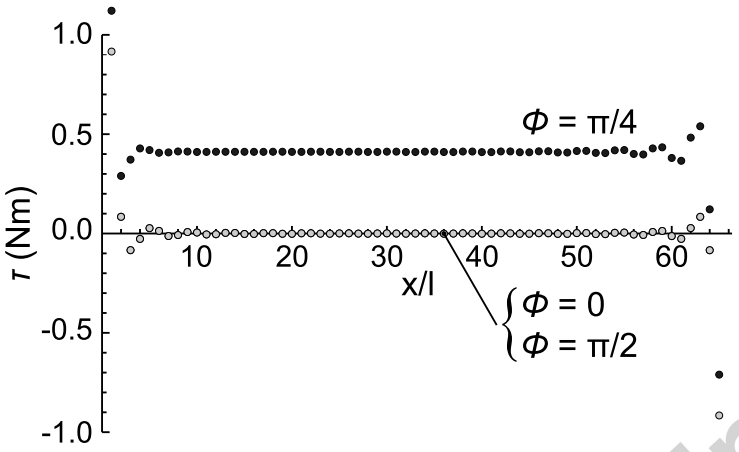

Figure 5: Torque on each dipole in the line dipole array at rotation angles $\phi = 0, \pi/4, \pi/2$ radians.

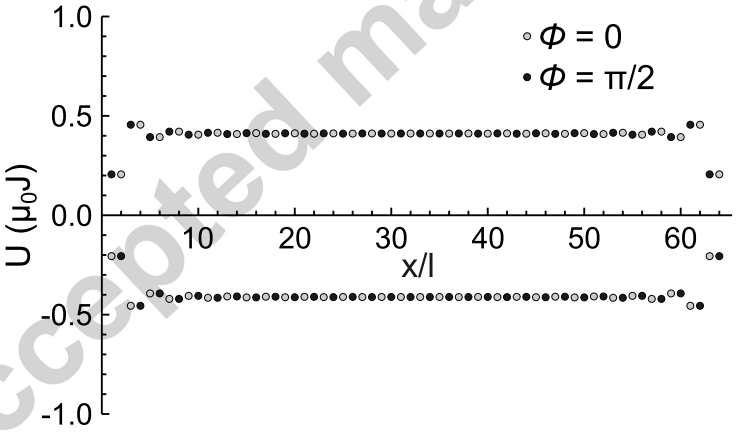

Figure 6: Energy of each dipole in the line dipole array at rotation angles $\phi = 0, \pi/4, \pi/2$ radians.

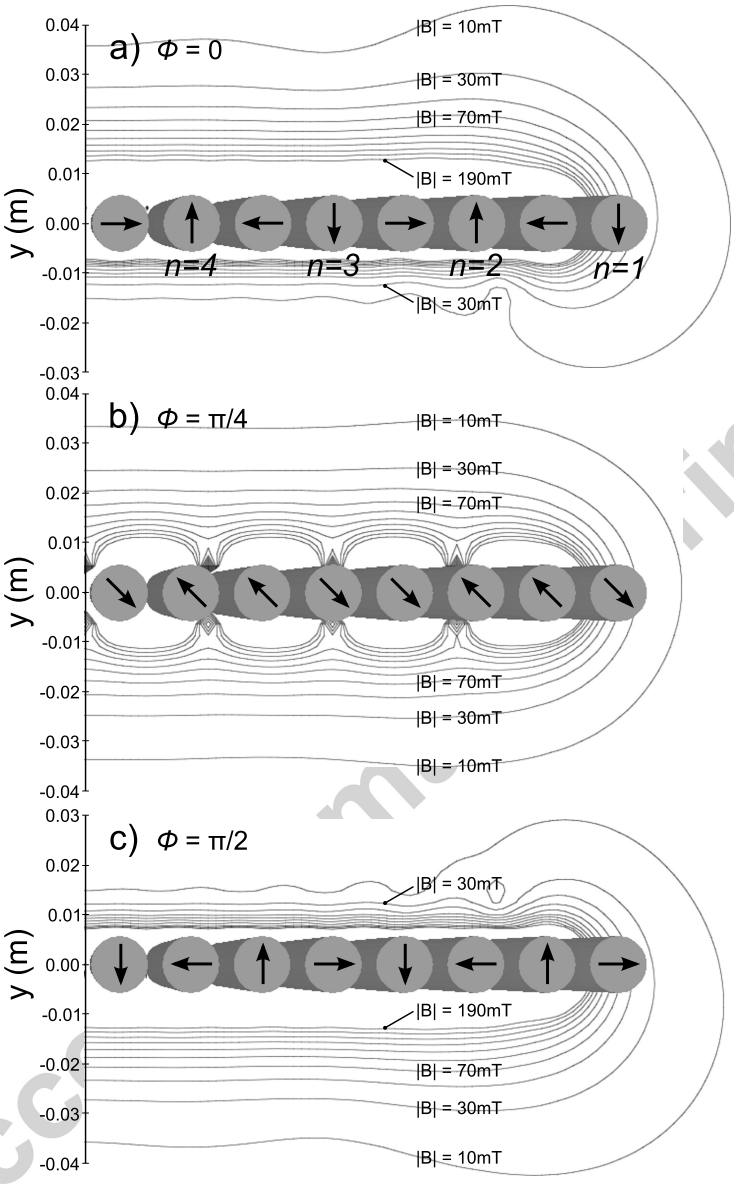

Figure 7: Flux density, $|\mathbf{B}|$ for array of magnetized rods, with rotations a) $\phi = 0$, b) $\phi = \pi/4$ and c) $\phi = \pi/2$ radians.

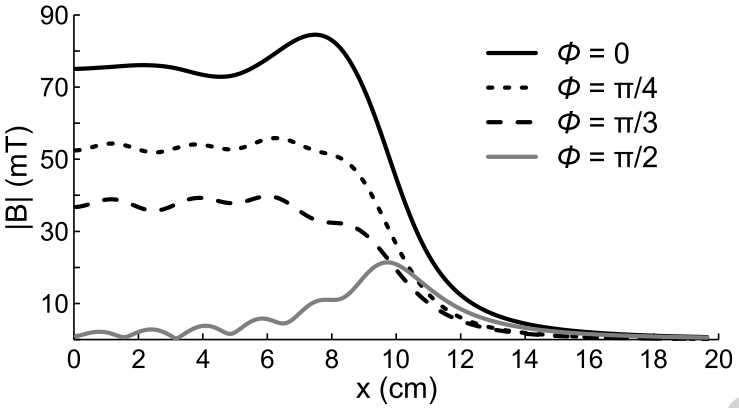

Figure 8: Flux density $|\mathbf{B}|$ against x along a line at $y = 2\ cm$, parallel to the x-axis, at rotation angles $\phi = 0, \pi/4, \pi/3, \pi/2$ radians.

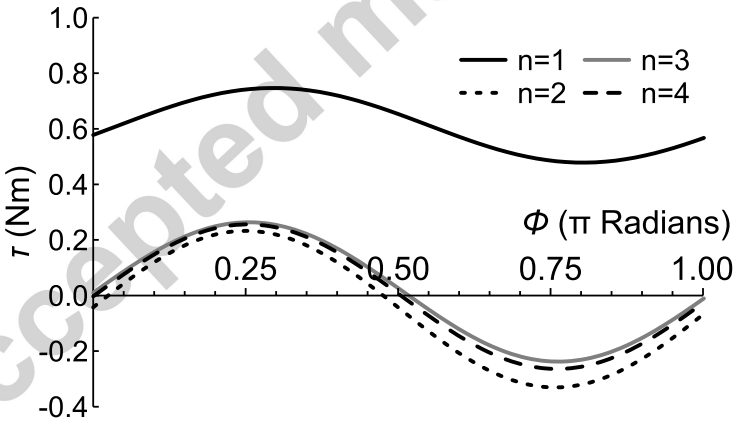

Figure 9: Torque on four rods in the design as a function of rotation angle ϕ.

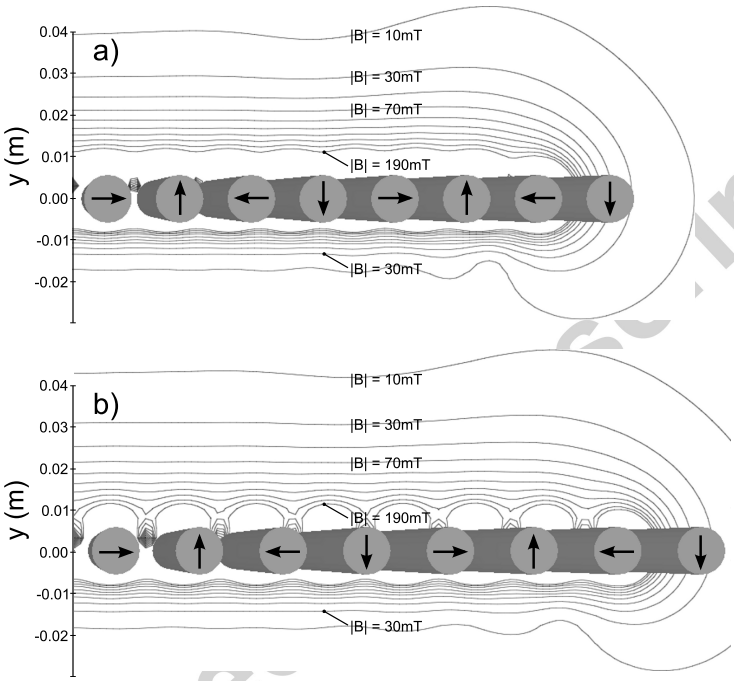

Figure 10: Flux density, $|\mathbf{B}|$ for array of magnetized rods, with $\phi = 0$ and spacing a) 50 mm and b) 75 mm.

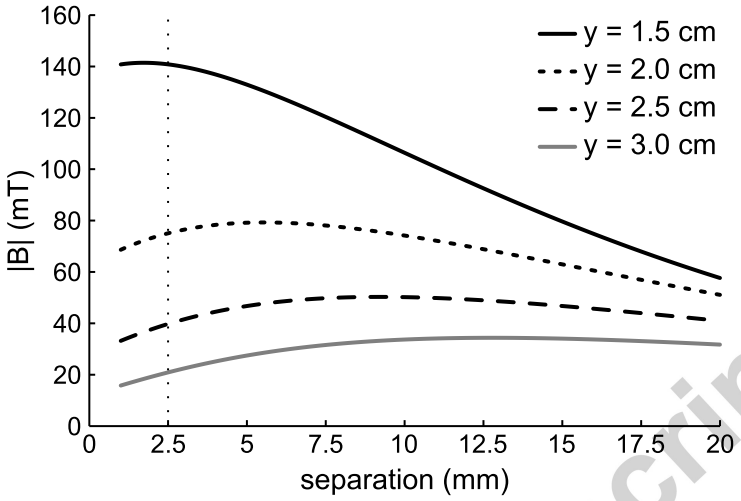

Figure 11: Flux density, $|\mathbf{B}|$, in the center of the array at four vertical positions as a function of rod separation.

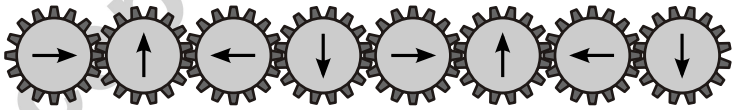

Figure 12: A straightforward implementation of the device using an equal mechanical gearing arrangement.

 We model an adjustable ‘one sided’ flux sheet made up of a series of dipolar magnetic field sources.

 We show that magnetic field can be switched from one side of sheet to other by an swap rotation of each of magnetic sources.

 Investigations show that such an arrangement is practical and can easily be fabricated.

 The design has a wide range of potential applications.